EXPERIMENTAL SHEAR TESTING OF TIMBER-MASONRY DRY CONNECTIONS

Authors: Daniele Riccadonna, Ivan Giongo, Gianni Schiro, Ermes Rizzi and Maria Adelaide Parisi

Corresponding author: Ivan Giongo ivan.giongo@unitn.it

ABSTRACT:

The mechanical coupling of timber products to the masonry walls of unreinforced masonry (URM) buildings is generating considerable interest in terms of seismic vulnerability mitigation. An extensive experimental investigation on timber panel to masonry wall connections realised with screw anchor fasteners is presented. A total of 64 shear tests under monotonic, cyclic and hemicyclic loading conditions were performed on site in a historic URM building. The examined parameters were: masonry type, timber panel product and material, load-to-grain direction, fastener geometry and steel grade. The outcomes of the campaign are then reported and discussed focusing on the strength and stiffness properties and on the dissipation capacity and residual strength of the connection under cyclic load. Moreover, a log-normal distribution fitting is proposed for the maximum load and slip modulus measurements of all the cyclic test configurations analysed. Finally, the principal experimental observations are listed along with recommendations for future work or use in practice.

KEYWORDS: masonry, retrofit, shear connections, CLT panel, LVL, screw anchor, seismic behaviour

1 INTRODUCTION

The seismic vulnerability is recognised as being the most important factor to consider in the design phase of structural strengthening systems for unreinforced masonry (URM) buildings. Recent earthquake events occurred in Italy ([1] and [2]) have shown that a change of the original use to situations implying higher loads along with improper interventions on historic masonry structures may lead to disproportionate damage levels. Given the importance of the subject, researchers have proposed a wide range of strengthening solutions for URM buildings over the last decades; with regard to the use of timber as reinforcing material two main approaches can be identified: a timber frame [3] or alternatively a timber panel [4] connected to the masonry walls by means of dowel-type fasteners which can be either grouted or screwed in the wall depending on the situation (Figure 1 reports a cross-sectional view of both the solutions). Preliminary work in the field of timber panel-to-masonry reinforcement was carried out by Sustersic and Duijc ([5] and [6]) investigating the use of cross laminated timber (CLT) panels as retrofitting solution for reinforced concrete (RC) frames with masonry infill. They proposed to place the timber panels on the external side of the building, fastened on the RC frame by means of steel brackets connected to both concrete and timber. In addition, they performed also tests on timber panels directly anchored to the masonry wall by means of epoxy grouted threaded steel rods. In recent years other researchers ([7] and [8]) extended the idea of seismic strengthening of URM buildings through CLT panels. In [7] Lucchini et al. proposed to insert timber panels in the internal side of the walls, connected through epoxy grouted threaded steel rods in order to preserve the original façade. Pozza et al [8] studied both the solutions in the external and internal side of the walls; in the former case the timber panels are fastened to a metallic curb anchored to the wall at the floor level, in the latter case the panels are connected to the floor by means of an L-shaped metallic curb.

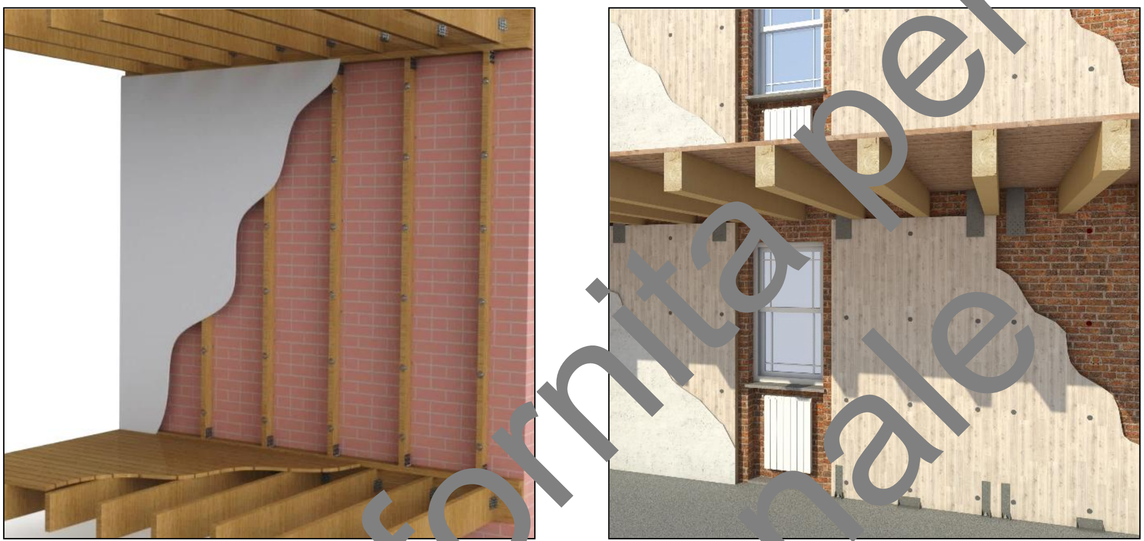

Figure 1 Schematic representation of retrofitting techniques of an URM building using timber strong-backs [3] and timber panels [4] connected to the internal side of the wall.

As pointed out in the reported literature review, a key aspect in the retrofitting of URM buildings by means of timber panels is the connection of the panels to the existing structures. In [4] the authors proposed to use dowel type fasteners (screws or bolts) to create a dry connection between the timber panel and the masonry wall. The advantages of this technique appear as manifold: the use of multiple fasteners distributed throughout the entire wall surface should ensure a certain amount of robustness toward localised damage or defects. The shear force transfer improves both the in-plane and out-of-plane behaviour of the wall-to-panel composite system. Moreover, screw type fasteners guarantee a complete reversibility of the refurbishment technique and a higher cost-effectiveness with respect to epoxy based connections.

The outcomes of an extensive experimental campaign on timber-masonry dry connections are reported here. Connections were realised with five different types of screw anchors technically approved for use in rock and concrete. A total of 64 shear tests were performed under monotonic, cyclic and hemicyclic load conditions. The research was carried out on the site of a historic URM building (dating back to the mid-19th century) located in northern Italy. Two types of masonry wall, made of stone and brick respectively, and three types of timber panels made from either softwood or hardwood species were selected for the experimental investigation. Three different load-to-grain angles, namely 0°, 45° and 90°, were examined assuming as grain direction the orientation of the timber panels with the maximum number of layers in the fibre direction.

2 TEST CONFIGURATION

This section describes the characteristics of the materials involved in the experimental campaign; for the timber elements and for the fasteners the data are referred to the corresponding technical approval provided by the producers, whereas for masonry preliminary tests were performed on small specimens collected from the building. In addition, the testing protocol and the experimental apparatus, based on similar campaigns described in the literature ([9]-[12]) are presented.

2.1 MATERIALS

Shear tests were carried out on two different types of masonry present in the historic four-storey URM building adopted as reference in this study. A series of 52 tests were performed on four brick masonry walls (Figure 2 right) located at the top floor, which date back to a period around 1910-1920, when one additional storey was raised on the original structure. The remaining 12 tests were conducted on two rubble masonry walls (Figure 2 left) made of coarse stone blocks (limestone and dolomite) and lime mortar.

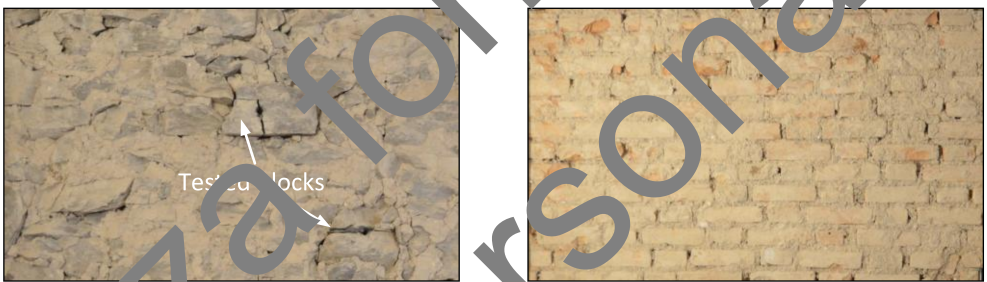

Figure 2 The two tested masonry typologies: stone masonry wall and brick masonry wall

Several small specimens, including mortar, bricks and stone blocks, were gathered from different places of the building and were tested in the laboratory of the University of Trento to check the quality of the masonry and characterize the principal mechanical properties. In particular, 15 bricks, 5 stone blocks and 30 mortar samples were tested under compression to determine the compression strength and the modulus of elasticity of the materials. The brick tensile strength was also derived from three-point bending tests [13]. The results in terms of mean values and coefficients of variation are reported in Table 1.

Table 1 Mechanical properties of the two tested masonry types according to the preliminary tests

Material characteristic			n° samples	Mean	CoV
Brick compression strength	f_{bc}	[N/mm^2]	15	14.83	0.32
Brick modulus of elasticity	E_{bc}	[N/mm^2]	15	1225	0.29
Brick bending tensile strength	f_{bt}	[N/mm^2]	7	3.70	0.43
Stone compression strength	f_{sc}	[N/mm^2]	5	64.30	0.33
Stone modulus of elasticity	E_{sc}	[N/mm^2]	5	7660	0.40
Mortar compression strength	$f_{mc,brick}$	[N/mm^2]	13	5.16	0.35

(brick masonry)					
Mortar compression strength (stone masonry)	$f_{mc,stone}$	[N/mm^2]	46	2.95	0.95

Table 2 details the main features of the five different fasteners chosen for the campaign according to the technical documentation and approval certificates supplied by the producers ([17]-[19]). As already stated in the introduction, all the fasteners were developed for the use in concrete as self-tapping screw anchors but are suitable for a whole range of other materials such as natural stone and brick. The assembly process is relatively simple: after drilling a pilot-hole the dust has to be removed and then the anchor can be fixed using a screw driver or a screw wrench. Fasteners M1 and M2 differ for insertion length in the masonry wall for a given panel thickness; fasteners M1 and U1 have comparable geometric properties but are produced by two different companies. Anchor U2 has the largest diameter of all (almost 14 mm over 10 mm). Lastly, fastener T is composed by two different threaded parts of equal length, one to be fixed in the masonry wall and the other in the timber panel. A detailed representation of the geometric properties of all the fasteners is provided in Figure 3.

Table 2 Geometric and mechanical properties of the fasteners according to the technical assessment given by the producers

Fastener type			M1 [17]	M2 [17]	U1 [18]	U2 [18]	T* [19]
Total length:	L	[mm]	180	240	160	150	160
Thread length:	L_t	[mm]	100	100	100	100	70 (70)
Thread diameter:	d_{thread}	[mm]	12.0	12.0	12.5	16.6	12 (14)
Core diameter:	d_{core}	[mm]	9.4	9.4	9.4	13.3	9.4 (9.5)
Shaft diameter:	d_{shaft}	[mm]	9.4	9.4	9.9	13.7	-
Head diameter:	d_{head}	[mm]	18	18	15	21	16
Washer diameter:	d_{washer}	[mm]	43	43	20**	28**	-
Axial resistance:	$N_{Rk,s}$	[kN]	25	25	55	103	25
Yielding moment:	$M_{y,k}$	[Nm]	38	38	95	269	38

* In brackets the timber thread properties

** Part of the fastener (see Figure 3)

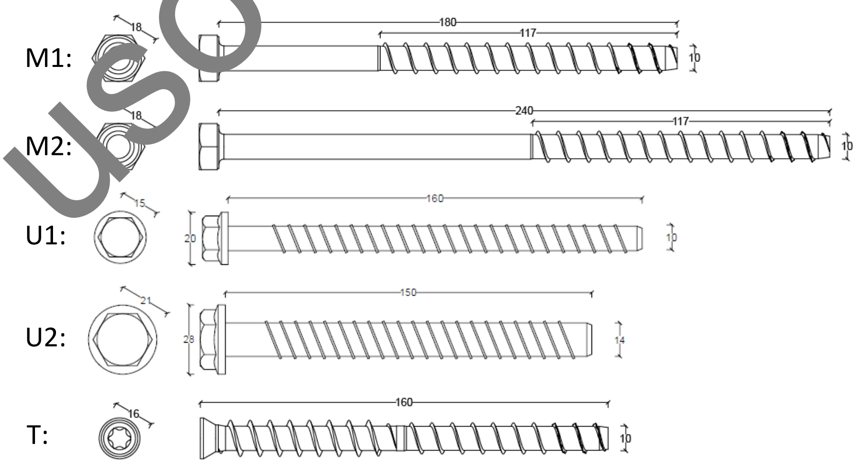

Figure 3 Representation of three of the five tested typologies of screw anchors adopted for the test

Due to the location of the timber panels at the internal side of the wall, their thickness should be kept to a minimum to avoid excessive loss of inner floor space. For this reason, one cross-laminated timber (CLT) and two laminated veneer lumber (LVL) panel types with a thickness respectively of 60 mm and 40 mm are selected for the tests. The mechanical properties of the panels are listed in Table 3; for the LVL elements only the in-plane bending properties are reported because the out-of-plane behaviour of the retrofitting solution is beyond the scope of the present paper.

Table 3 Strength and stiffness properties of the timber elements according to the standards

Element type			Spruce CLT Panel [14]	Spruce LVL Panel* [15]	Beech LVL Panel* [16]
Bending:	$f_{m,0,k}$	[N/mm^2]	24	32	60
	$f_{m,90,k}$	[N/mm^2]	-	[illegible]	10
Tension:	$f_{t,0,k}$	[N/mm^2]	14.5	18	51
	$f_{t,90,k}$	[N/mm^2]	0.12	[illegible]	[illegible]
Compression:	$f_{c,0,k}$	[N/mm^2]	21	30	[illegible]
	$f_{c,90,k}$	[N/mm^2]	2.5	9	19
Shear:	$f_{v,k}$	[N/mm^2]	[illegible]	4.6	[illegible]
MoE:	$E_{0,mean}$	[N/mm^2]	[illegible]	10600	[illegible]
Shear modulus:	G_{mean}	[N/mm^2]	450	600	820
Density:	ρ_{mean}	[kg/m^3]	[illegible]	[illegible]	800
	ρ_k	[kg/m^3]	350	[illegible]	730
Thickness	t	[mm]	60	40	40

* In-plane bending properties

2.2 SET-UP AND TESTING PROTOCOL

The details of the experimental apparatus adopted for the campaign are shown in Figure 4. Firstly, a rectangular timber reaction frame was fixed on the selected masonry wall using the same screw anchors (fastener T) of the shear tests. The hydraulic actuator used to apply the shear load was secured to one timber post of the frame by means of a C-shaped steel bracket. The specimen under test was primarily connected to the wall driving the anchor through the pre-drilled pilot hole in the brick/stone block using a 5 mm thick spacer in the back side of the timber panel. The specimen was joined to the actuator through a hinged union interposing a 75 kN load cell. To prevent in-plane and out-of-plane rotations of the specimen during the push phase of the cyclic testing, two steel angle brackets were attached to the reaction frame. Strips of polyzene were positioned in the internal side of the steel angle brackets in order to reduce the friction between the steel-to-steel surface. Lastly, a linear variable differential transducer (LVDT) was used to monitor the displacement of the timber specimen with respect to the masonry wall. The base of the LVDT was placed on a sturdy steel support fixed on the floor; this allowed to disregard the (minimal) reaction frame deformability in the calculation of the fastener stiffness.

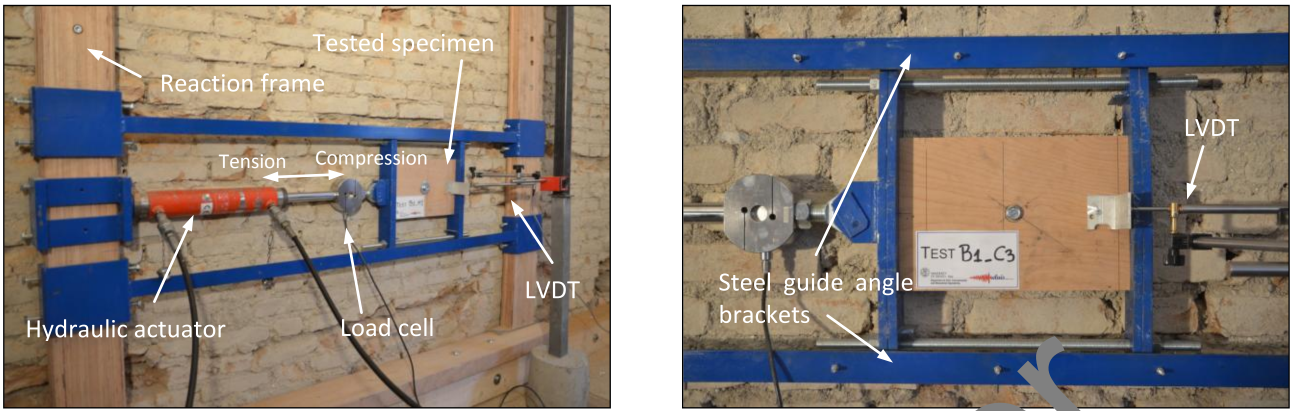

Figure 4 Test set-up details and instruments arrangement

With reference to the testing procedure, both monotonic and cyclic behaviours were investigated. The load was applied in displacement control up to a maximum displacement of 50 and 30 mm for the monotonic and for the cyclic tests, respectively. In particular, testing protocols of EN 26891 [20] and EN 12512 [21] were followed; the monotonic tests (EN 26891) provided the yield displacements required to perform the complete procedure of cyclic testing (EN 12512). In addition, the standard ASTM E2126 [22] was employed to plot the envelope curves starting from the total load-displacement hysteresis loops and, from the envelope curves, to determine the equivalent energy elastic plastic (EEEP) curves both for tension and compression loads (see Figure 5 right).

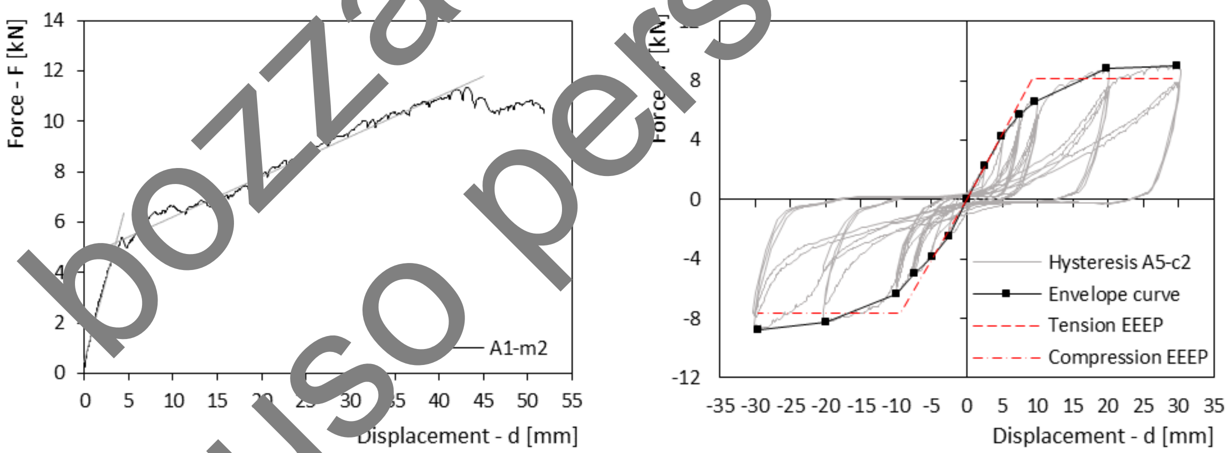

Figure 5 Typical load-displacement curves of a monotonic test (left) and of a cyclic test (right)

Table 4 reports all the tested configurations, selected varying the type of masonry, timber panel and fastener and considering different load-to-grain angles. For all the tests performed with fastener M1 and M2 in combination with softwood panels (either CLT or LVL), a 38 mm wide and 4 mm thick washer was used to enable the formation of the second plastic hinge. In the case of beech LVL panels a first trial monotonic test was executed without using the washer; because no significant timber damage was observed around the fastener head, it was decided to perform all the tests including beech LVL panels without washer. Fasteners U1 and U2 are produced with a built-in washer (Table 2 and Figure 3); therefore, it was also assumed unnecessary to use an external washer.

Table 4 Configurations of the 64 shear tests performed

Test ID	n° repetitions		Masonry type	Timber panel		Fastener
	Monotonic	Cyclic		Material	α* [°]	
A1	1	3	Brick	Spruce CLT	0°	T
A2	1	3	Brick	Spruce CLT	90°	T
A3	1	3	Brick	Spruce CLT	45°	T
A4	2	3	Brick	Spruce CLT	0°	M1+washer
A5	2	3	Brick	Spruce CLT	0°	M2+washer
A8	1	3	Brick	Spruce CLT	0°	U2
A9		3	Brick	Spruce CLT	0°	U1
B1	1	3	Brick	Beech LVL	0°	M1
B2	1	3	Brick	Beech LVL	90°	M1
B3		3	Brick	Beech LVL	0°	U2
D1	2	3	Stone	Spruce CLT	0°	M1+washer
D2		3	Stone	Spruce CLT	0°	T
D3	1	3	Stone	Spruce CLT	0°	U2
E1	1	3	Brick	Spruce LVL	0°	M1+washer
E2	1	3	Brick	Spruce LVL	90°	M1+washer
E3**	1	3	Brick	Spruce LVL	0°	T

* Load-to-grain angle (grain: maximum number of layers in the fibre direction)
** Panel thickness: 60 mm

3 RESULTS

3.1 OBSERVED FAILURE MODES

After the execution of each test (either monotonic or cyclic), the load and the displacement were returned to zero and the fastener was removed to evaluate the failure modes of the connection. Similar to other tests reported in literature on shear dowels embedded in stone masonry [12], partial or total splitting of either bricks and stone blocks was experienced in almost all the tests (Figure 6 and Figure 7). Only in the case of rubble stone masonry some of the blocks (test D1-m1, D1-m2, D3-m1 and D3-c2) remained undamaged whereas the surrounding mortar underwent a complete crushing (see Figure 7-D). This was probably related to the poor mechanical performance of the lime-mortar (see Table 1) and/or to the local excessive thickness of the mortar joints. This phenomenon is reflected in the load-displacement curves of the tests, characterised by a relative low value of slip modulus (< 0.5 kN/mm) and an almost linear behaviour.

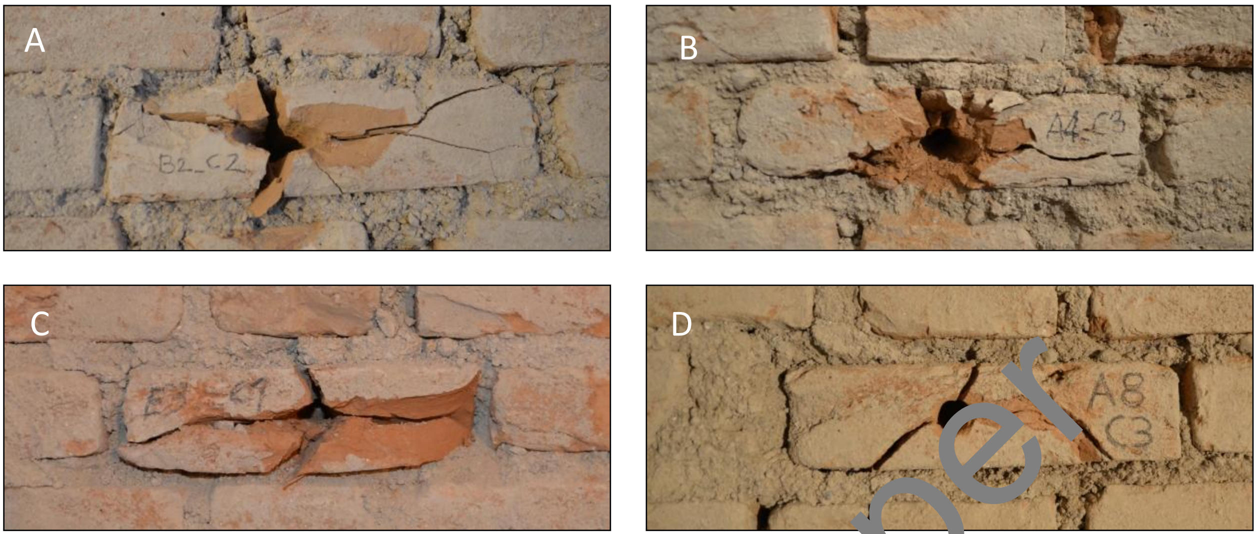

Figure 6 Observed damage for the brick masonry: A brick tensile cracking, B local crushing, C brick splitting, D early failure due to pre-existing cracks (test interrupted and discarded)

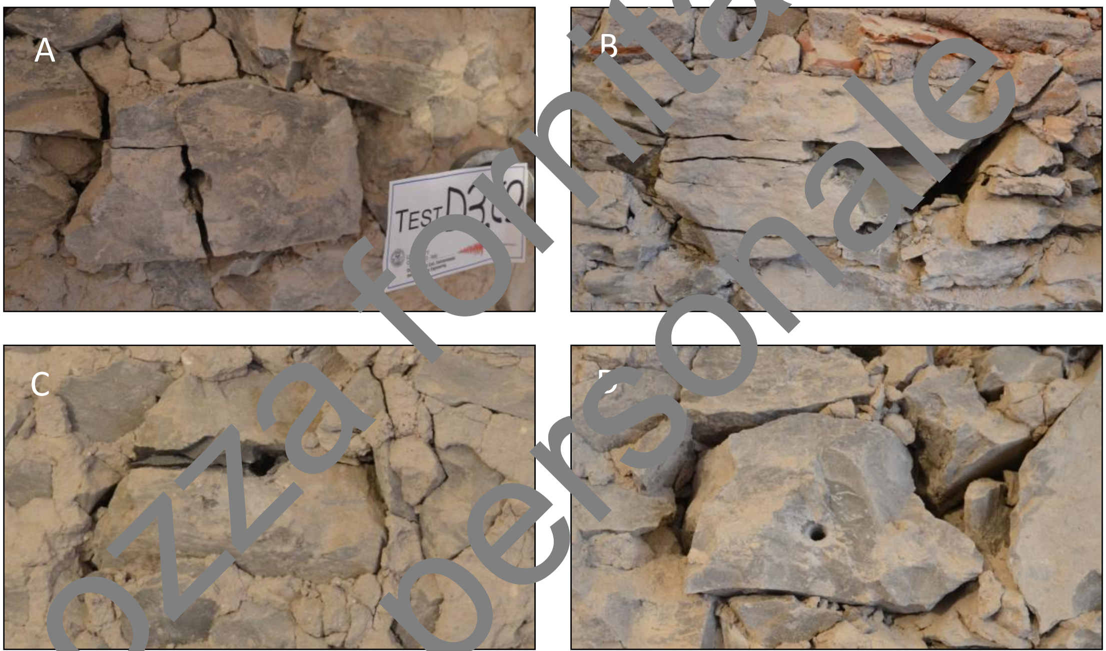

Figure 7 Observed damage for the rubble stone masonry: A block tension cracking, B analogous of a “plug shear” failure, C block splitting, D mortar crushing

Figure 8 presents the graphs of two cyclic tests (test A1-c3 and A3-c1) and a schematic representation of the brick condition during the loading phases. The three principal damage conditions observed for brick masonry tests are represented: brick cracking (tension), crushing (compression) and splitting. When the cracks started to open, the response curves showed a sudden, yet limited, capacity loss (Figure 8a) that did not correspond to the actual failure of the connection as the capacity continued to increase. Conversely, when crushing of the brick around the fastener becomes noticeable (usually accompanied also by timber bearing failure and plastic hinge/hinges formation in the fastener), the load is approaching the maximum load carrying capacity of the connection. The second and more dangerous type of failure is the splitting of the brick, namely the opening of a crack parallel to the load direction. This was experienced only in a few specimens and generally at large displacement values (d > 15 mm). The splitting failure of the brick caused an almost total loss of capacity of the connection since there was no more material opposing the movement of the fastener. The (small) residual capacity might be due to the compression within the masonry wall which tended to hold the brick portions together after the splitting. It is worth reminding that the risk of splitting is minimum when the predrill hole is at the centre of the brick, while it increases moving towards the edges.

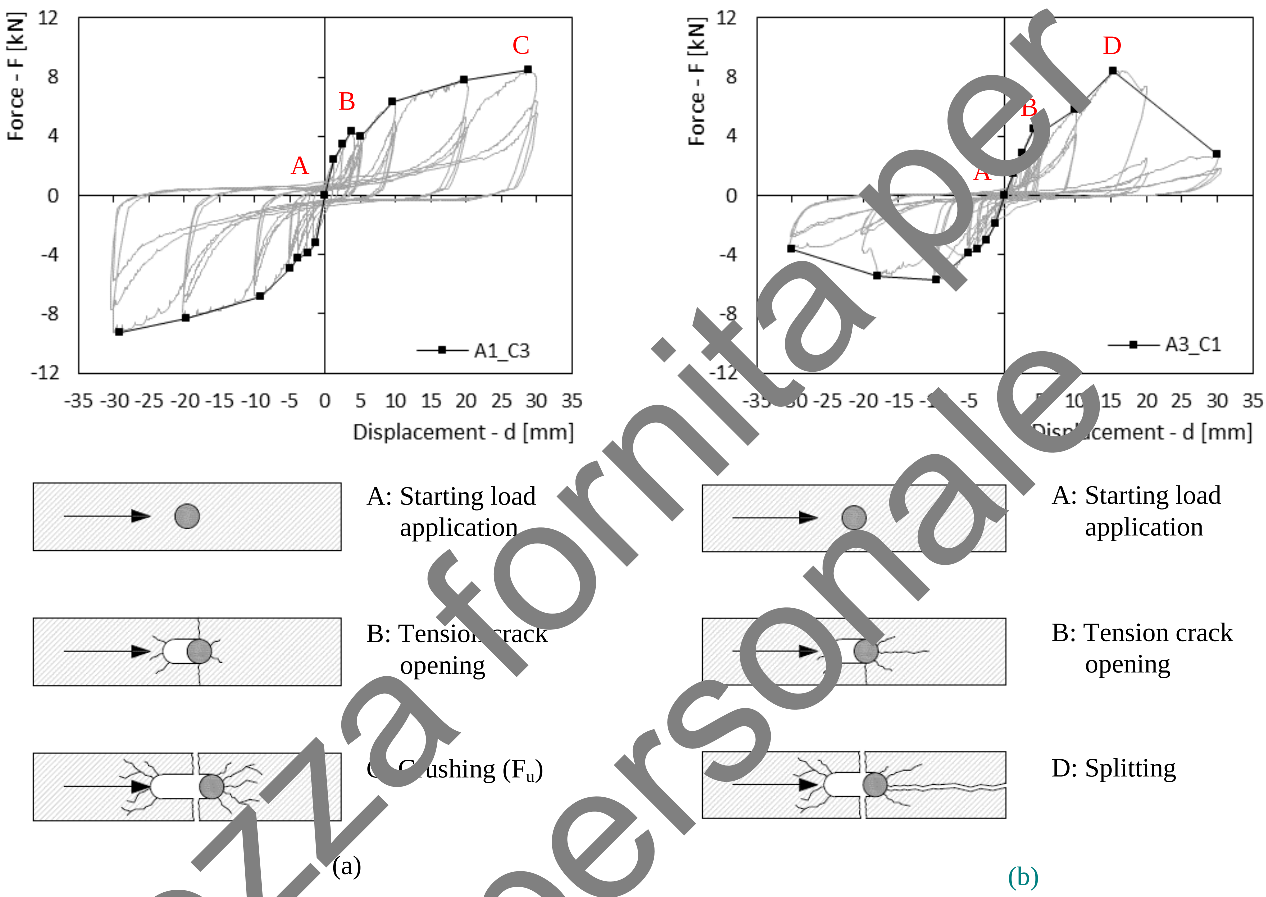

Figure 8 Representations of two different failure modes (compression crushing (a) and splitting (b)) observed for the specimens on brick masonry walls

With the exception of the few tests previously mentioned where crushing of the mortar surrounding the stone block was observed and the test configurations involving U2 fasteners (A8, B3 and D3), all the tests developed at least one plastic hinge inside the masonry in the fastener portion closer to the wall surface (Figure 9 left). U2 fasteners showed a higher value of characteristic yielding moment ($M_{y,k}$ = 269 Nm, see Table 2) compared to the other fasteners with the consequence that the plastic hinges did not activate during the tests. As expected, in single threaded fasteners (M1, M2 and U1) the first plastic hinge originated at the top of the threaded part inserted in the masonry wall; in the case of monotonic loading, also a second plastic hinge, formed in the timber element due to the presence of the washer, was clearly distinguishable from the anchors recovered after the end of the tests. For the cyclic tests the presence of the second plastic hinge was not as evident as for the monotonic tests, probably due to lower maximum displacement value and to the return to the zero values of load and displacement which may have straightened back the fastener shank. Double threaded fasteners (T) formed a single plastic hinge located at the interface between the masonry wall and the timber panel and exhibited marked timber crushing also in correspondence with the fastener head. A brittle tensile rupture of the screw anchor shank was experienced only once, in test D1-c3 (Figure 9 right). The maximum load recorded during this test was the highest of the whole campaign (F_{max} = 18.29 kN). Failure of the screw shank in tension was calculated from the product data sheet as equal to 25.0 kN which is less than the 10.4 kN determined for the washer pull-through resistance (it is worth noting that no embedment of the washer was observed). This may have been caused by weakening of the fastener due to oligocyclic fatigue.

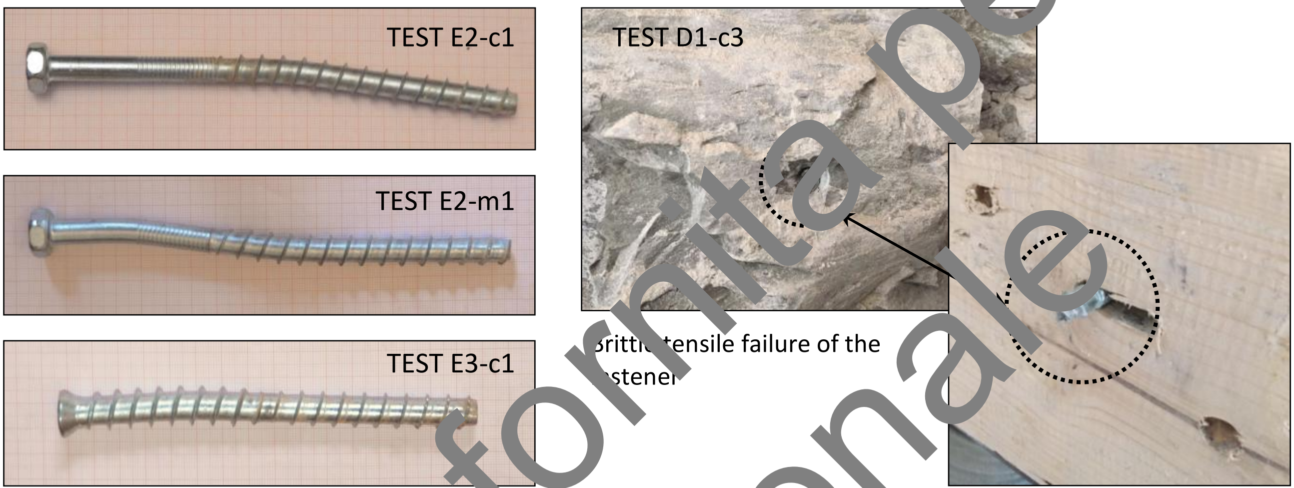

Figure 9 Examples of plastic hinges from the fasteners removed after the tests (left) and tensile rupture registered for test D1-c3 inserted in stone masonry (right)

Due to the irreversible nature of the splitting failure of bricks and stone blocks and of the timber crushing of the wood panels, a significant level of pinching appears from the load-displacement curves of the cyclic tests, particularly for the hysteresis loops at relatively large displacement amplitudes (i.e. d = 10 mm, 20 mm and 30 mm). Therefore, in the second and third cycles the only contribution to energy dissipation is provided by the yielding of the steel fastener. For this reason, connections with fasteners that have a smaller value of yield moment may exhibit less pinching, thanks to the lower energy required to activate the plastic hinge (this was confirmed by the results as shown in Figure 10).

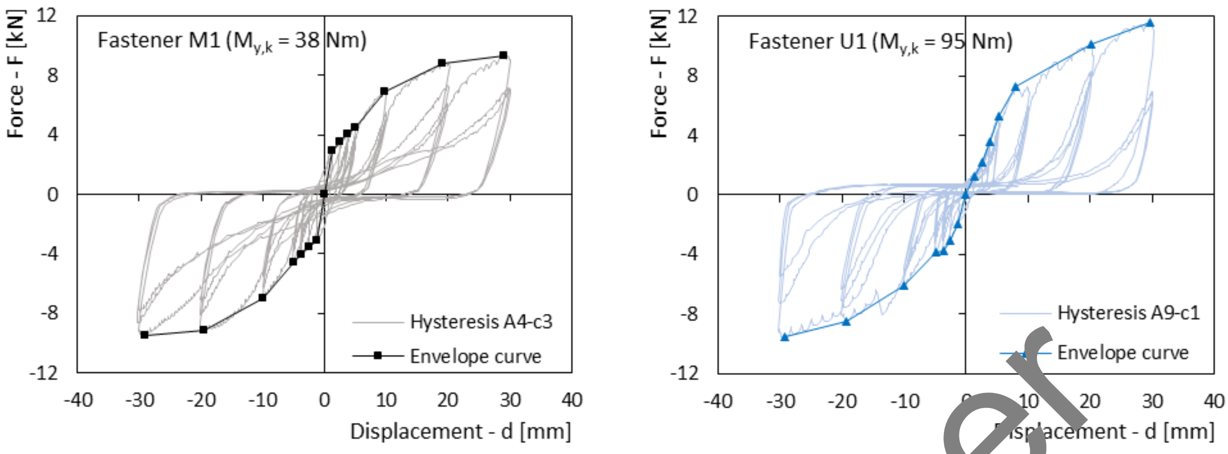

Figure 10 Hysteresis loops of test A4-c3 (fastener M1) and test A9-c1 (fastener U1)

Due to the large number of specimens tested on brick masonry, it was not possible to carry out the whole campaign on a single wall. Consequently, three brick masonry walls, located in three different areas of the building, were chosen for the experimental investigation (Table 5 details the position of every single cyclic and hemicyclic test on brick masonry).

Table 5 Location of each cyclic and hemicyclic test performed on brick masonry wall

Test ID	Wall	Test ID	Wall	Test ID	Wall
A1-c1	W1	A5-c2	W1	B2-c3	W1
A1-c2	W1	A5-hc3	W3	B3-c1	W2
A1-c3	W1	A8-c1	W1	B3-hc2	W3
A2-c1	W1	A8-c2	W1	B3-hc3	W3
A2-hc2	W3	A8-hc3	W3	E1-c1	W2
A2-hc3	W3	A9-c1	W2	E1-c2	W2
A3-hc1	W2	A9-hc2	W3	E1-c3	W2
A3-hc2	W3	A9-hc3	W3	E2-c1	W2
A3-hc3	W3	B1-c1	W1	E2-c2	W2
A4-c1	W1	B1-c2	W1	E2-hc3	W3
A4-c2	W1	B1-c3	W1	E3-c1	W2
A4-c3	W1	B2-c1	W1	E3-c2	W2
A5-c1	W1	B2-c2	W1	E3-hc3	W3

The connection showed a tendency to strength and stiffness reduction in the tests executed on wall W3; in a visual inspection, several brick blocks in W3 displayed signs of defects and inclusions (e.g. excessive porosity, grains of burnt limestone or grogs). For this reason, it was decided to carry out a complementary non-destructive testing (NDT) campaign on the three selected walls, to supplement the material test results reported in Table 1. In particular, the scleroscopic method was adopted, using a Schmidt impact hammer according to EN 12504-2 [23]. This technique had been already applied on brick masonry by other authors [24] who effectively identified an almost linear relation between the measured rebound number from the NDT test and the compression strength of the block. Twenty-four measurements for each wall were collected on randomly selected intact brick blocks; the frequency distributions of the rebound number are shown in

Figure 11. It can be observed that wall W3 exhibited lower values of rebound number, a possible sign of decreased mechanical properties.

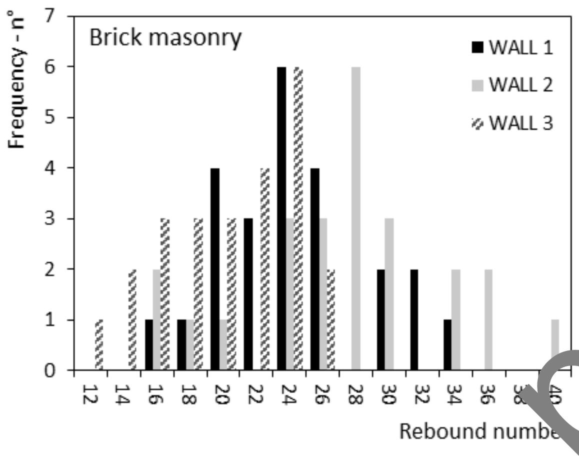

Figure 11 Frequency distributions of the rebound number measured via sclerоscopic test method on the three tested walls

3.2 MONOTONIC TESTING

This section reports the results of the monotonic loading tests. As stated before, all the monotonic tests were loaded (in tension) up to a displacement value of 50 mm (except for tests B1-m1 and B2-m1). Figure 12 shows the load-displacement curves for the spruce CLT panel and brick masonry combination, on the left using the fastener T and varying the load-to-grain angle and on the right maintaining the load parallel to the grain of the outer layers of the panel using different types of fastener. The different inclination of the load with respect to the grain direction of the CLT panel seems to have no impact on the mechanical behaviour of the connection (this was also confirmed by the corresponding cyclic tests). The graph on the right exhibits, instead, a more pronounced variety of results. It is worth noting that using a steel fastener with larger diameter and higher yielding moment (e.g. fastener U2) leads to poorer mechanical performance of the overall connection. This may be due to failure on the masonry side: a much stiffer steel dowel exerts excessive pressure on the brick leading to preliminary failure, as shown by the early loss of strength of the load-displacement curve. Furthermore, the need of a wider pilot-hole may have contributed to weaken the brick element.

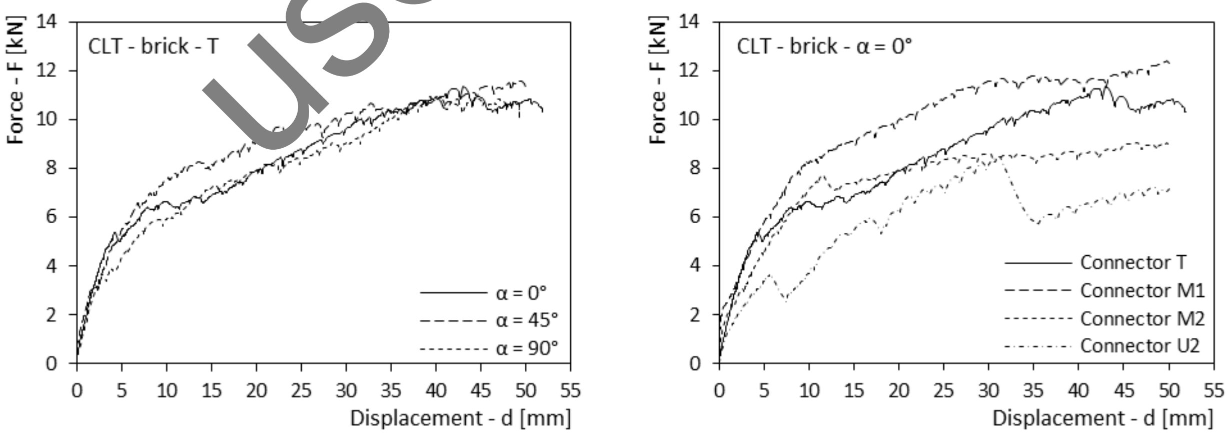

Figure 12 Selected load-displacement curves for different load-to-grain angles (left) and for different types of fasteners (right)

Table 6 summarises the results of each monotonic test, in terms of maximum load, yield point and slip modulus. For tests A8-m1, D1-m1, D1-m2, D3-m1 and E3-m1 the yield point was not calculated because of early failure of the masonry due to cracking of the brick and/or block (A8-m1 and E3-m1) or due to crushing of the surrounding mortar (D1-m1, D1-m2 and D3-m1). This latter phenomenon also resulted in relatively low values of slip modulus because the stone blocks were free to translate in the first phase of the monotonic tests. Unlike spruce CLT panels, beech LVL specimens (tests B1-m1 and B2-m1) showed larger sensitivity to testing in different load-to-grain angles. The test perpendicular to the main fibre direction (B2-m1) exhibited a 27.5% decrease in the maximum load decrease and a 71.7% reduction of the slip modulus with respect to test parallel to the main fibre (B1-m1). This behaviour may be due to the lower percentage of orthogonal layers in the beech LVL (2 over a total of 14 lamellae for a 40 mm thick panel) compared to spruce CLT. The results for spruce LVL panels tested with different load-to-grain angle (E1-m1 and E2-m1) were similar to those of beech LVL panels: the test parallel to the grain recorded higher maximum load (+32.2%) and higher slip modulus (+73.5%) with respect to the panel tested orthogonal to the main fibre direction.

Table 6 Maximum load, yield point and slip modulus of all the monotonic tests performed

Test ID	Maximum load F_{max} [kN]	Yield point F_y [kN]	Yield point d_y [mm]	Slip modulus k_s [kN/mm]
A1-m2	11.35	5.18	[illegible]	1.31
A2-m1	10.94	[illegible]	7.38	0.75
A3-m1	11.58	7.67	6.70	1.02
A4-m1	12.39	[illegible]	6.41	0.99
A4-m2	11.94	[illegible]	6.82	0.74
A5-m1	9.06	7.02	7.80	0.80
A5-m2	8.89	[illegible]	10.11	0.62
A8-m1	[illegible]	-	-	0.70
B1-m1*	[illegible]	7.75	3.75	1.77
B2-m1*	9.32	5.34	9.19	0.50
D1-m1	12.70	-	-	0.24
D1-m2	18.10	-	-	0.33
D3-m1	15.61	-	-	0.42
E1-m1	15.12	6.45	3.54	1.44
E2-m1	11.44	5.41	5.11	0.83
E3-m1	9.72	-	-	0.43

* Tested up to 30 mm

3.3 CYCLIC TESTING

The cyclic test protocol was calibrated according to EN 12512 [21]. The yield displacement derived from the monotonic testing, was equal to 5 mm for all the configurations with the exception of test A5 (fastener M2) where it was set at 10 mm. The cyclic tests were performed up to a displacement amplitude of 30 mm both in tension and compression loading (in the graphs the tension and compression loads will be reported in the positive and negative axis, respectively). The examined parameters were:

- Type of fastener (different diameter, length, steel and typology);
- Load-to-grain direction (0°, 45° and 90°);
- Type of timber panel (spruce CLT, spruce LVL and beech LVL);
- Type of masonry (brick masonry, rubble stone masonry).

Table 7 reports the principal parameters that characterise the envelope curves of each considered configuration: peak load, slip modulus (calculated according to EN 26981 [20]) and the yielding load of the equivalent energy elastic-plastic curve associated to the envelope curve [22]. The mean value and coefficient of variation (corresponding to three repetitions for each test) are listed, keeping the tension and compression hemicycles as separate.

Table 7 Mean value and coefficient of variation of the maximum load, slip modulus and yield load (determined using the EEEP curve according to [22]) of the envelope curves for each cyclic test configuration

Test ID	Load	F_{max} [kN]		k_s [kN/mm]		$F_{y,EEEP}$ [kN]	
		Mean	CoV	Mean	CoV	Mean	CoV
A1	Tension	7.96	[illegible]	1.11	28.6%	[illegible]	3.3%
	Compression	8.52	[illegible]	1.61	[illegible]	[illegible]	15.1%
A2	Tension	7.45	[illegible]	0.84	[illegible]	6.13	7.2%
	Compression	[illegible]	[illegible]	0.75	[illegible]	5.99	1.2%
A3	Tension	7.40	13.9%	0.80	[illegible]	5.69	1.2%
	Compression	5.73	-	1.33	-	4.86	-
A4	Tension	8.91	4.0%	0.91	27.6%	7.82	3.2%
	Compression	[illegible]	4.8%	[illegible]	41.5%	8.02	7.0%
A5	Tension	8.20	9.8%	[illegible]	33.6%	6.13	11.9%
	Compression	7.99	9.7%	0.80	1.1%	6.95	10.6%
A8	Tension	9.34	[illegible]	1.32	79.2%	8.56	15.4%
	Compression	9.87	[illegible]	0.60	12.1%	8.44	3.3%
A9	Tension	8.38	[illegible]	1.06	5.5%	7.08	36.0%
	Compression	[illegible]	-	0.86	-	7.97	-
B1	Tension	10.25	[illegible]	3.94	33.2%	8.85	4.1%
	Compression	12.30	10.0%	1.38	14.0%	9.92	14.5%
B2	Tension	[illegible]	7.9%	1.08	28.8%	7.27	8.9%
	Compression	8.99	19.2%	0.51	15.2%	7.72	20.2%
B3	Tension	12.64	7.3%	1.28	12.3%	10.95	9.1%
	Compression	11.71	-	0.85	-	10.93	-
D1	Tension	12.64	14.4%	1.18	45.0%	11.13	14.5%
	Compression	14.98	20.9%	1.54	21.3%	12.30	27.5%
D2	Tension	6.57	8.4%	0.84	41.0%	5.74	13.4%
	Compression	5.52	0.3%	0.35	16.4%	4.89	9.0%
D3	Tension	9.80	11.1%	2.30	60.5%	8.75	2.6%
	Compression	11.95	37.2%	0.80	49.6%	10.59	36.6%
E1	Tension	9.29	12.8%	1.42	31.2%	7.51	15.3%
	Compression	9.41	5.8%	2.10	61.5%	7.69	6.3%
E2	Tension	7.85	18.5%	1.33	67.4%	6.54	15.1%
	Compression	7.73	22.2%	0.93	47.6%	6.42	23.8%
E3	Tension	8.26	6.3%	0.86	30.8%	6.73	10.2%
	Compression	7.50	17.6%	1.28	41.6%	6.36	22.8%

Other important aspects to consider in a cyclic test concern the strength reduction of the connection from the first to the third cycle at the same displacement amplitude, and the energy dissipation of the joint during the hysteresis cycles. Usually, the impairment of strength ΔF and equivalent viscous damping ratio ν_{eq} (according to EN 12512 [21]) are used to describe such qualities. Table 8 and Table 9 summarize the ΔF data in terms of percentage reduction with respect to the first loop at the same displacement amplitude and the ν_{eq} data (complete cycles comprehending tension and compression loading).

Table 8 Cyclic tests: mean values and coefficients of variation of the impairment of strength ΔF at increasing levels of displacement

Test ID	ΔF [%]	0.75 d_y*	1 d_y*	2 d_y*	4 d_y*	6 d_y*
Total loop n°		5	8	11	[illegible]	17
A1	Mean	20%	18%	24%	28%	31%
	CoV	0.43	0.38	0.16	0.34	0.22
A2	Mean	20%	14%	21%	27%	35%
	CoV	0.18	0.86	0.50	0.21	0.28
A3	Mean	37%	26%	[illegible]	58%	32%
	CoV	0.32	0.29	[illegible]	0.32	[illegible]
A4	Mean	18%	16%	[illegible]	22%	22%
	CoV	0.29	0.30	0.23	0.27	[illegible]
A5**	Mean	27%	22%	30%	17%	[illegible]
	CoV	0.47	0.42	0.31	0.34	[illegible]
A8	Mean	28%	[illegible]	15%	[illegible]	[illegible]
	CoV	0.36	0.39	0.52	0.42	0.40
A9	Mean	15%	21%	21%	30%	39%
	CoV	0.57	0.30	[illegible]	[illegible]	0.19
B1	Mean	22%	20%	[illegible]	26%	39%
	CoV	0.47	0.43	0.38	0.37	0.16
B2	Mean	15%	22%	20%	24%	29%
	CoV	0.55	[illegible]	[illegible]	0.25	0.23
B3	Mean	28%	34%	27%	37%	41%
	CoV	0.10	0.25	0.25	0.25	0.20
D1	Mean	20%	20%	35%	34%	37%
	CoV	[illegible]	0.33	0.39	0.21	0.54
D2	Mean	[illegible]	8%	16%	20%	21%
	CoV	0.40	0.63	0.76	0.74	0.65
D3	Mean	14%	18%	28%	48%	47%
	CoV	0.61	0.40	0.44	0.25	0.32
E1	Mean	22%	30%	32%	29%	32%
	CoV	0.08	0.39	0.12	0.19	0.38
E2	Mean	21%	19%	25%	34%	25%
	CoV	0.30	0.41	0.44	0.33	0.55
E3	Mean	26%	29%	26%	42%	32%
	CoV	0.63	0.80	0.44	0.33	0.25

* Relative to the third loop
** Different yield displacement (d_y=10 mm instead of 5 mm)

Table 9 Cyclic tests: mean values and coefficients of variation of the equivalent viscous damping ratios ν_{eq} at increasing levels of displacement

Test ID	ν_{eq} [%]	0.25 d_y	0.50 d_y	0.75 d_y*	1 d_y*	2 d_y*	4 d_y*	6 d_y*
Total loop n°		1	2	5	8	11	14	17
A1	Mean	22.3%	18.3%	9.8%	7.5%	6.2%	7.3%	8.5%
	CoV	0.16	0.11	0.30	0.23	0.24	0.21	0.32

A2	Mean	12.9%	10.7%	6.2%	4.9%	3.7%	4.8%	4.3%
	CoV	0.18	0.19	0.24	0.22	0.59	0.13	0.15
A3	Mean	18.5%	11.8%	8.5%	8.0%	10.2%	5.0%	5.3%
	CoV	0.22	0.15	0.09	0.38	0.67	0.48	0.54
A4	Mean	33.1%	24.1%	10.7%	7.3%	5.3%	7.1%	10.0%
	CoV	0.14	0.14	0.10	0.09	0.15	0.20	0.09
A5**	Mean	19.4%	13.4%	6.0%	5.1%	5.1%	6.9%	0.0%
	CoV	0.11	0.10	0.20	0.33	0.51	0.45	0.00
A8	Mean	32.6%	22.4%	13.2%	10.1%	6.0%	5.1%	6.6%
	CoV	0.08	0.11	0.55	0.60	0.37	0.33	0.46
A9	Mean	24.4%	18.8%	9.8%	8.3%	4.1%	4.8%	4.7%
	CoV	0.14	0.07	0.14	0.24	0.16	0.16	0.34
B1	Mean	30.2%	21.4%	11.1%	8.0%	7.2%	9.8%	12.0%
	CoV	0.07	0.06	0.30	0.23	0.33	[illegible]	0.13
B2	Mean	21.1%	19.2%	9.9%	8.4%	5.8%	[illegible]	9.9%
	CoV	0.27	0.17	0.20	0.18	0.27	0.37	0.25
B3	Mean	24.8%	15.1%	4.7%	3.6%	[illegible]	2.1%	4.6%
	CoV	0.29	0.23	0.32	0.26	[illegible]	0.33	0.69
D1	Mean	24.2%	19.7%	12.6%	11.0%	9.3%	9.5%	8.8%
	CoV	0.16	0.22	0.36	0.32	0.10	0.09	0.28
D2	Mean	19.9%	14.0%	9.5%	[illegible]	[illegible]	9.0%	6.9%
	CoV	0.24	0.18	0.12	0.13	0.24	0.40	0.31
D3	Mean	21.2%	18.4%	12.4%	[illegible]	9.0%	7.7%	9.9%
	CoV	0.31	0.26	0.05	[illegible]	0.16	[illegible]	0.17
E1	Mean	32.2%	21.4%	[illegible]	[illegible]	4.7%	[illegible]	5.3%
	CoV	0.12	0.03	[illegible]	0.18	0.21	[illegible]	0.16
E2	Mean	27.4%	22.0%	11.8%	8.1%	5.6%	[illegible]	5.0%
	CoV	0.02	0.18	0.31	0.29	0.19	0.44	0.37
E3	Mean	19.2%	[illegible]	[illegible]	8.8%	5.4%	5.0%	5.9%
	CoV	0.09	0.14	0.20	0.18	0.28	0.47	0.60

* Relative to the third loop
** Different yielding displacement (d_y=[illegible] mm instead of 5 mm)

Influence of the type of fastener

The influence of the type of fastener was investigated by selecting the following wall-panel combination: brick masonry wall and spruce CLT panel loaded parallel to the main grain direction. Fasteners T, M1, M2, U2 and U1 were tested in configurations A1, A4, A5, A8 and A9, respectively. As pointed out in Table 7, all the tests exhibited comparable mean values of maximum capacity and different (mean values of the slip modulus (either between different tests or between tension and compression hemicycles of the same configuration, CoV of F_{max} considering all configurations equal to 16.41% and CoV of k_s equal to 50.13 %)). The larger scatter observed for the slip moduli may be explained by reminding that the calculation method is based on the secant stiffness values measured at 0.1 F_{max} and 0.4 F_{max} (EN 26891), which is the force range where the tension cracking of the bricks occurred (for the specimen that exhibited cracking). Therefore, the early loss of strength caused higher variability of the slip modulus, whereas the more stable values of maximum capacity may be correlated to the compression strength of the brick blocks and the embedment strength of the timber panels, almost uniform for all the configurations analysed in this section (see Figure 8 left).

The connection capacity and slip modulus of the envelope curves appear governed more by the mechanical properties of the masonry walls and timber panels than by the choice of fastener typology. One exception may be the use of a fastener with large diameter (e.g. fastener U2 → test A8) which may cause early failure due to the weakening of the block (net resisting area reduction) affecting the slip modulus (tension cracking) or even the ultimate load (splitting). When looking at the impairment of strength values and equivalent viscous damping ratios (Table 8 and Table 9) a more marked difference among fasteners stands out. In particular, two groups may be distinguished on the base of the steel type: zinc plated steel (fasteners T, M1 and M2) and zinc plated hardened carbon steel (fasteners U1 and U2). The latter group exhibited higher strength loss and smaller equivalent viscous damping ratios for displacements greater than 10 mm. This is linked to the more pronounced pinching experienced by hardened carbon steel anchors, with respect to normal steel anchors (see Figure 10). The higher yield moment of hardened carbon steel anchors (M_{yk} = 95 Nm and M_{yk} = 269 Nm for fasteners U1 and U2 with respect to M_{yk} = 38 Nm for fasteners T, M1 and M2) delayed or even inhibited the formation of the plastic hinge on the fastener, reducing the amount of energy dissipation of the second and third loops for the cyclic loading conditions.

Influence of the load-to-grain direction

The considered load-to-grain direction angles were:

- 0°, 45° and 90° for softwood CLT panel, brick masonry wall and fastener T (test configuration A1, A2 and A3 respectively);
- 0° and 90° for hardwood LVL panel, brick masonry wall and fastener M1 (test configuration B1 and B2 respectively);
- 0° and 90° for softwood LVL panel, brick masonry wall and fastener M1 (test configuration E1 and E2 respectively);

As already observed in the monotonic loading tests (section 3.2), CLT panels manifested quite consistent mechanical behaviour in terms of maximum load and slip modulus, independently from the loading direction. Nonetheless, the best performance is usually obtained for load parallel to the main grain direction of the panel (α = 0°). The smaller maximum capacity obtained for the 45° configuration (test A3) was due to the splitting of the block and was not linked to the load-to-grain direction. On the contrary, LVL panels (either realised with beech or spruce lumber) exhibited a clearer distinction between specimens loaded parallel or perpendicular to the main fibre direction of the panels (≈20% capacity variation); as for the monotonic tests, the 90° load-to grain angle configurations presented the lowest ultimate strength and slip modulus values. The different response between CLT and LVL panels seems to be attributable to the smaller percentage of orthogonal layers in the LVL panels with respect to the whole panel thickness (14% for hardwood LVL, 14% and 20% for softwood LVL panels with thickness of 40 mm and 60 mm, respectively, and 33% for spruce CLT) which is directly related to the embedment strength.

Influence of the type of timber panel

Figure 13 presents the comparison among different timber panels while maintaining constant the other connection parameters. The figure reports on the left the results for the tests performed with fastener M1 (test configuration A4, B1 and E1 for softwood CLT, hardwood LVL and softwood LVL panels) and on the right the results for the tests performed with fastener T (test configuration A1 and E3 for softwood CLT and softwood LVL panels). Also tests with fastener U2 were carried out on brick masonry using both softwood CLT panels and beech LVL panels (tests configuration A8 and B3), but the graphs are not reported here for sake of brevity (for the outcomes discussion refer to Table 7, Table 8 and Table 9). Typically, specimens realised with softwood CLT or softwood LVL showed similar performances whereas connections assembled using beech LVL panels exhibited an increase both in maximum load capacity and slip modulus value (despite of the minor thickness of beech LVL panels). This seems to confirm the hypothesis that the governing property on the timber side is the embedment strength of the wood, which depends mainly on the density of the material. Being softwood CLT and softwood LVL panels both obtained from the same wood species, they have comparable values of embedment strength (≈ 40 MPa), whereas the higher density of beech hardwood is reflected by a higher value of the embedment strength (> 60 MPa).

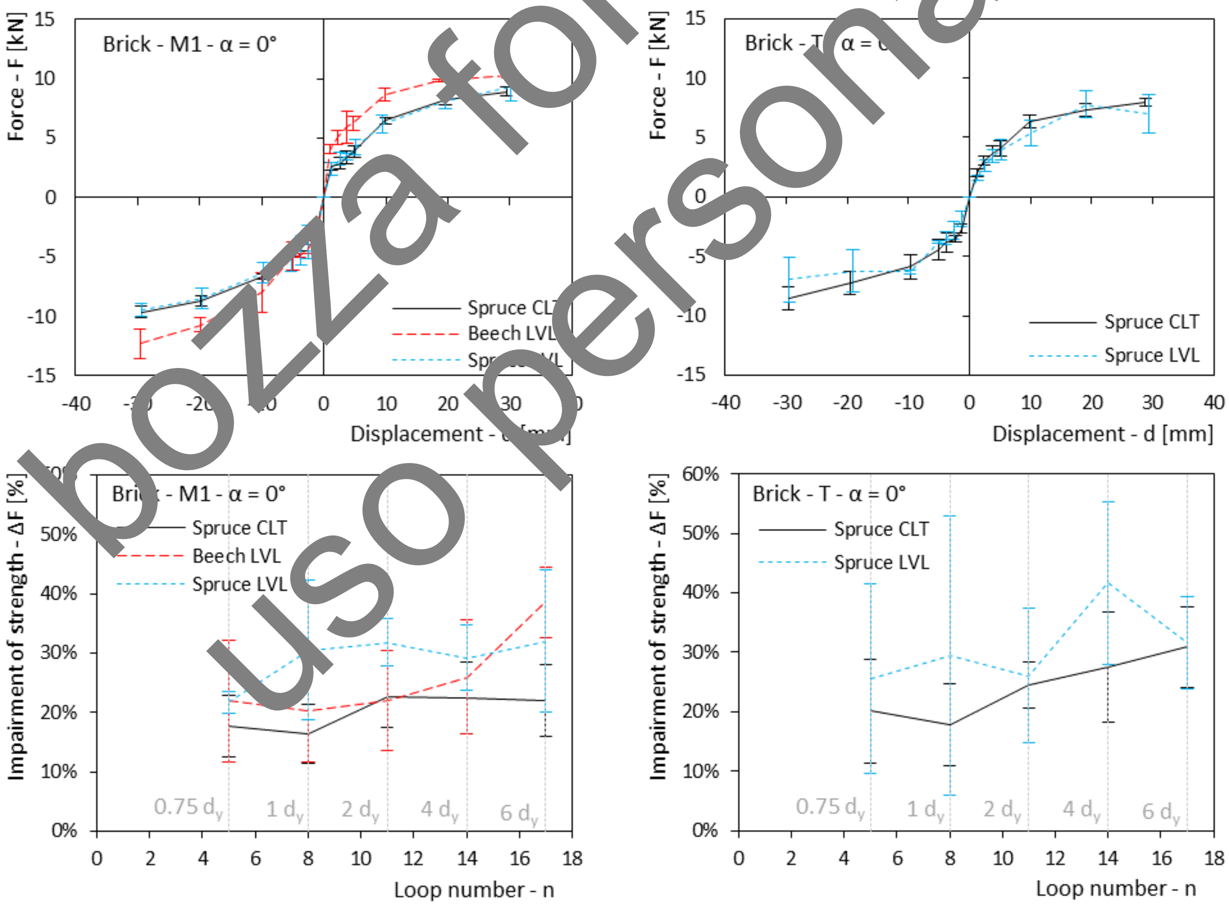

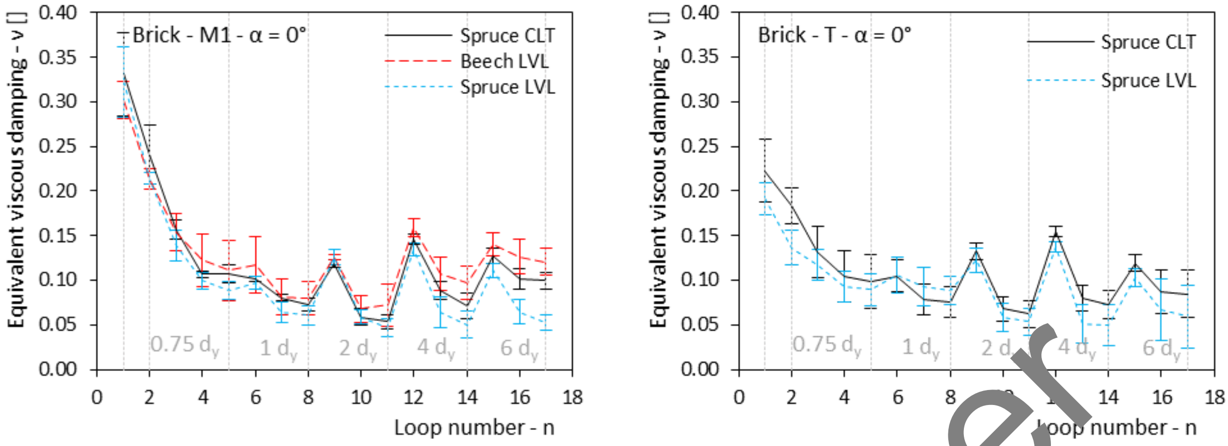

Figure 13 Mean envelope curves, impairment of strength and equivalent viscous damping (including standard deviations: error bars) of fasteners M1 (left) and T (right) for brick masonry and α equal to 0° varying the type of timber panel

Influence of the type of masonry

For comparing the two masonry typologies, the test configuration couples A4-D1, A1-D2 and A8-D3 can be examined (corresponding, respectively, to fasteners M1, T and U2 connecting spruce CLT panels with brick and stone masonry walls). Not surprisingly, tests performed on the stone masonry (i.e. D1, D2 and D3 configurations) exhibited higher maximum capacity and stiffness than tests performed on brick masonry (i.e. A1, A4 and A8 configurations). However, they displayed also more scattered results due to the higher variability of the rubble stone masonry pattern (block dimensions, thickness of mortar joints, etc.). In addition, a preferential crack propagation direction was observed in the failure modes of stone masonry (see Figure 7). This phenomenon may be due to the sedimentary nature of most of the rocks composing the masonry walls: the stratigraphy of various superimposed layers of sediments determines an orthotropic behaviour of the final material (rock) with smaller tensile strength in the direction perpendicular to the layers. Focusing on the hysteretic properties at small displacement levels, stone masonry manifested lower equivalent viscous damping ratios than brick masonry (Figure 14, last two graphs). A possible explanation can be found in the higher hardness of the stone blocks compared to clay brick blocks: at small displacements, the softer brick larger deformation and early cracking allow greater energy dissipation. As the displacement increases, the dissipation property of the connection is more dependent on the fastener typology, therefore the divergence of the equivalent viscous damping ratio between stone and brick masonry tends to decrease.

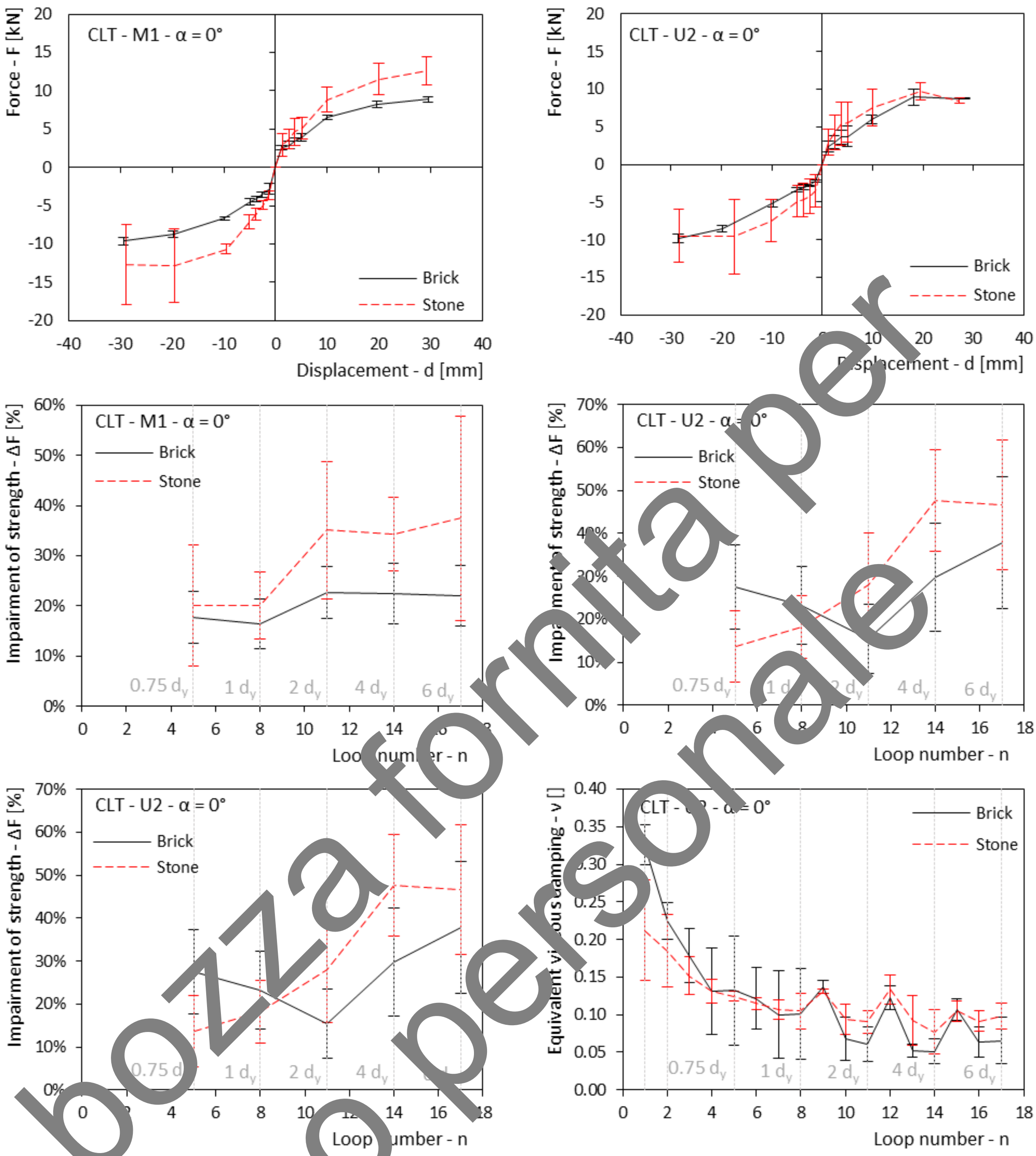

Figure 14 Mean envelope curves, impairment of strength and equivalent viscous damping (plus standard deviations: error bars) of fasteners M1 (left) and U2 (right) for CLT timber panels and α equal to 0° varying the masonry type

General remarks

For all the cyclic and hemicyclic tests, the maximum connection capacity was limited by the local failure of the masonry (with the exception of test D1-c3 where a brittle failure of the steel anchor shank was experienced). Depending on the type of masonry failure (tension, splitting, compression crushing, mortar crushing, etc.) the maximum load and the slip modulus were subjected to consistent variation. For such reason, in order to determine upper bound and lower bound limits for both the capacity and the stiffness of dry timber-masonry connections, a statistical analysis of the maximum load values and the slip moduli was carried out. Firstly, the frequency distributions of the maximum load and of the slip modulus were calculated separating the tension and compression hemicycles and assuming discrete intervals of 0.5 kN and 0.25 kN/mm for the maximum load and slip modulus respectively (Figure 15).

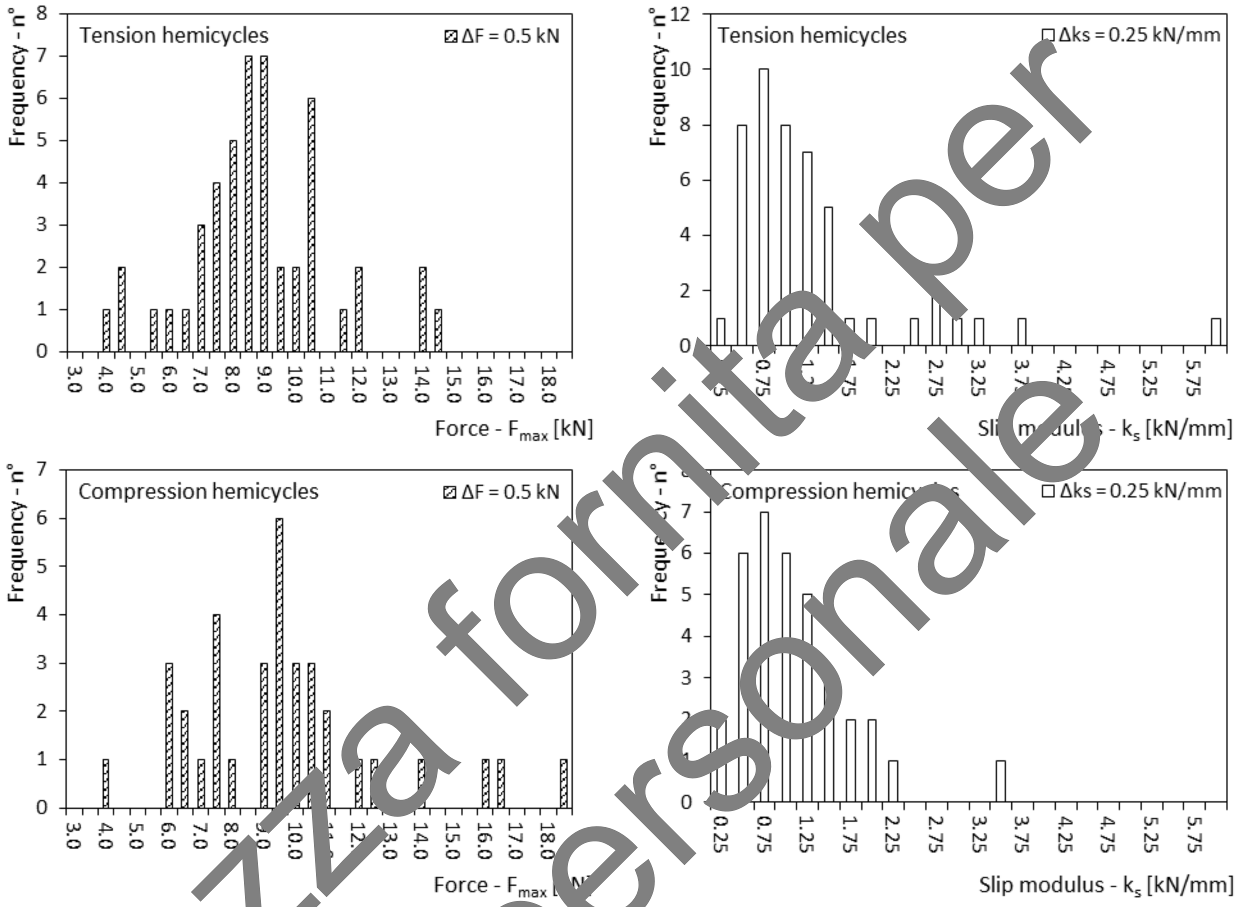

Figure 15 Statistical frequency analysis of all the 48 cyclic tests performed (divided in tension and compression hemicycles) of the maximum load (ΔF = 0.5 kN) and of the slip modulus (Δk_s = 0.25 kN/mm)

Table 10 lists the statistical moments of all the cyclic tests from the first moment, namely the expected value or mean of the sample, to the fourth standardised moment, specifically the kurtosis of the sample (also the excess kurtosis is reported). The third standardised moment (skewness) and the fourth standardised moment (kurtosis) are generally considered as shape indicator of the sample distribution. Both the maximum load and the slip modulus distribution exhibit positive values for the skewness, meaning that the distributions are skewed to the right. Also the excess kurtosis presents positive values; the distributions with positive excess kurtosis, called leptokurtic, have heavier tails with respect to the normal distribution. However, these two moments might be considered only as rough indicators of the true shape distribution of the population due to the limited size of the sample.

Table 10 Statistical moments of the tension hemicycles, compression hemicycles

Moment		Tension hemicycles		Compression hemicycles		Total	
		F_{max} [kN]	k_s [kN/mm]	F_{max} [kN]	k_s [kN/mm]	F_{max} [kN]	k_s [kN/mm]
Expected value	μ_1	8.60	1.22	9.38	0.99	8.93	1.12
Variance	m_2	4.94	1.04	9.72	0.41	7.10	0.79
Skewness	m_3	0.29	2.39	0.92	1.59	0.86	2.51
Excess kurtosis	m_4	0.62	7.61	1.28	4.26	1.75	9.07

Figure 16 shows the distribution fitting for the maximum load (right) and slip modulus (left) in terms of both probability density function and cumulative probability function. The fitting is performed using the method of moments and selecting a lognormal distribution due to the right skewed and leptokurtic nature of the experimental data. The method of moments approach simply adopts the sample mean and variance of the sample as estimators of the population mean and variance; from this equivalence the parameters of the selected distribution can be determined.

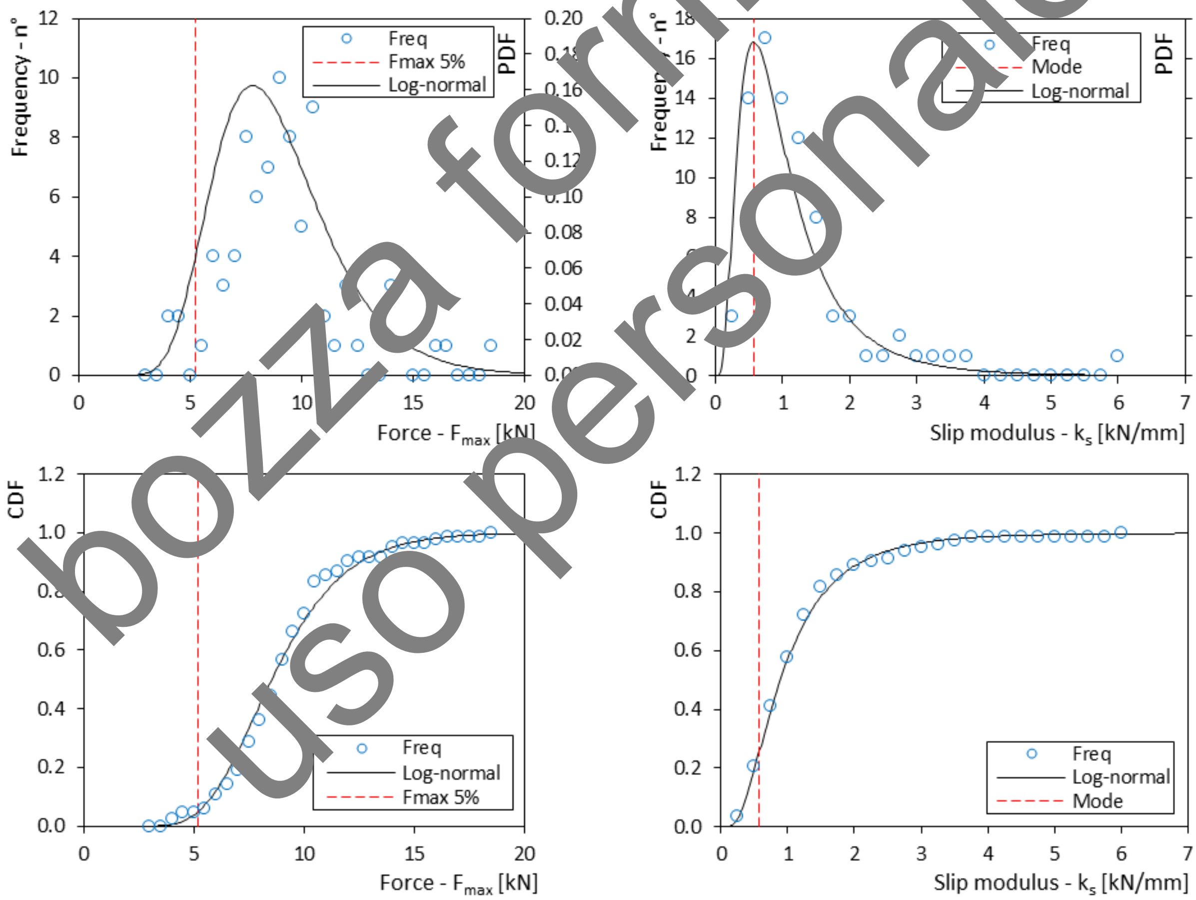

Figure 16 Lognormal distribution fitted to the data (both for tension and compression hemicycles) of load F_{max} (left) and slip modulus k_s (right) and representation of load characteristic value (5%) and slip modulus mode value

As an estimation of the goodness of fit the Shapiro-Wilk expanded test for log-normality was. The null-hypothesis of the test is that the population is log-normally distributed. If that is the case, then the p-values are expected to be greater than the selected cutoff (or significance level) α. The calculated p-values are 0.102 and 0.837 for the maximum load and the slip modulus distribution. Therefore, assuming a significance α level equal to 0.05, the null-hypothesis cannot be rejected with a confidence of 10.2% and 83.7% respectively. In addition, also the quantile-quantile (Q-Q) plots are reported in Figure 17 for a graphical validation of the goodness of fit of the chosen distributions.

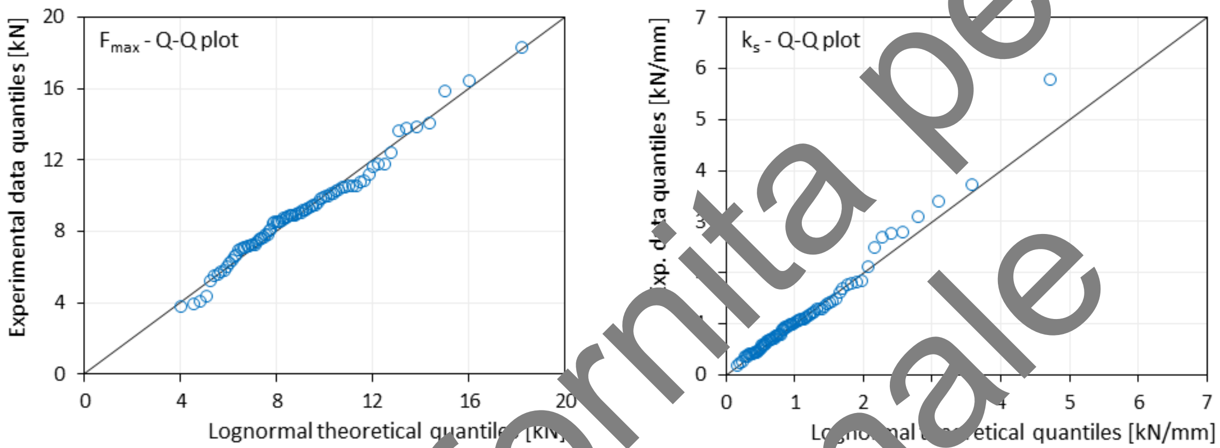

Figure 17 Quantile-Quantile plot of load F_{max} (left) and slip modulus k_s (right) fitted to a lognormal distribution

4 CONCLUSIONS

An extensive experimental investigation on timber panel to masonry wall dry connections was undertaken to evaluate the mechanical performance of the connections under static and seismic shear loading conditions. The tests were performed in an existing URM building, which dates back to the late 1800s, adopting monotonic, cyclic and hemicyclic loading protocols. Two different masonry typologies (brick masonry and rubble stone masonry) and three different timber panels (spruce CLT, spruce LVL and beech LVL) were selected for the campaign. The majority of the tests were carried out with a load-to-grain angle of 0° (load parallel to the main grain direction of the wood panel); nevertheless, also the 45° and the 90° load-to-grain directions were examined for the three types of timber panels. Lastly, five different screw anchor fasteners were used, with variable geometry (diameter, length, threaded parts, etc.) and material (mild steel and hardened carbon steel). In summary, the main outcomes of the study can be listed as follow:

- Connections on stone masonry walls exhibited higher mean values of maximum capacity and slip modulus with respect to the corresponding configuration on brick masonry walls, but also higher variability in the failure modes linked to a higher variability in the single test results. This may be attributed to the inconsistency of the rubble stone masonry patterns (block dimensions, thickness of the mortar joints, etc.).

- From the timber point of view, the identified key property in determining the connection capacity and stiffness, not surprisingly, was the embedment strength of the material. Therefore, the use of hardwood LVL increases both the capacity and the stiffness of the connection compared to softwood based material. Specimens realised with softwood CLT and softwood LVL showed similar performance, indicating that the product type has less influence on the mechanical properties of the connection with respect to the timber species or grade.
- The tests performed with different load-to-grain angles (α = 0°, 45° and 90°) suggest that the connections built with CLT panels are less sensible to the force direction. On the contrary, the specimens realised with LVL panels (either using spruce or beech wood) manifested a non-negligible reduction in both maximum load capacity and slip modulus. This distinction may be a consequence of the smaller percentage of lamellae and/or veneers in the perpendicular direction for the LVL compensated panel compared to the CLT panel (respectively equal to 14% and 33% of the whole thickness of the element).
- The choice of fastener typology seems to have lower impact on the strength and stiffness parameters of the connection in comparison with the selection of timber panel products or masonry wall elements. It is worth reminding that higher strength values of the masonry constituents might determine a stronger engagement of the fastener properties and result in an increased influence of the fastener typology. It is, however, advisable to use mild steel fasteners on brick masonry walls due to the increased energy dissipation of the connection under cyclic loading (earlier formation of the plastic hinge). On the other hand, for stone masonry walls the adoption of hardened carbon steel fasteners can reduce the risk of brittle tensile failure.
- As indicative reference values for estimating the shear performance of screw anchors connecting timber based panels to masonry walls, a capacity of 9.0 kN on average and a mean slip modulus equal to 1.1 kN/mm may be assumed. If required, different percentile values may be calculated from the proposed probability distribution used for fitting the reported experimental data. However, the validity range of the above mentioned values is limited to masonry support with characteristics comparable to those of the case study presented herein.

ACKNOWLEDGEMENTS

The authors gratefully thank Terme di Comano (IT) thermal consortium for providing building access and availability to undertake the testing campaign. The authors wish to thank Eng. Davide Galvanin, Eng. Marco Carlet and Eng. Stefano Segatta for their precious help during the experimental campaign. The research work was carried out within the framework of the 2018 ReLUIS-DPC network (Italian University Network of Seismic Engineering Laboratories and Italian Civil Protection Agency). Rubner Holzbau S.r.l., Pollmeir GmbH, Steico GmbH, Heco Italia EFG S.r.l. and Fischer Italia S.r.l. are gratefully acknowledged by the authors for supplying the material used for realizing the test specimens.

REFERENCES

[1] L. Sorrentino, S. Cattari, F. da Porto, G. Magenes and A. Penna "Seismic behaviour of ordinary masonry buildings during the 2016 central Italy earthquakes" *Bulletin of Earthquake Engineering*, 2018.

[2] G. Fiorentino, A. Forte, E. Pagano, F. Sabetta, C. Baggio, D. Lavorato, C. Nuti and S. Santini "Damage patterns in the town of Amatrice after August 24th 2016 Central Italy earthquakes" *Bulletin of Earthquake Engineering*, 2018.

[3] D. Dizhur, M. Giaretton, I. Giongo and J. M. Ingham "Seismic retrofit of masonry walls using timber strong-backs" *Journal of the Structural Engineering Society of New Zealand Inc*, vol. 30, no. 2, pp 30-44, 2017.

[4] I. Giongo, G. Schiro and M. Piazza "On the use of timber-based panels for the seismic retrofit of masonry structures" Proceedings of the 3rd International Conference on Protection of Historical Constructions (PROHITECH), Lisbon, Portugal, 2017.

[5] I. Sustersic and B. Dujic "Seismic strengthening of existing buildings with cross laminated timber panels" Proceedings of the World Conference on Timber Engineering (WCTE), Auckland, New Zealand, 2012.

[6] I. Sustersic and B. Dujic "Seismic shaking table testing of a reinforced concrete frame with masonry infill strengthened with cross laminated timber panels" Proceedings of the World Conference on Timber Engineering (WCTE), Quebec City, Canada, 2014.

[7] A. Lucchini, E. S. Mazzucchelli, S. Mangialardo and M. Persello "Façadism and CLT technology: An innovative system for masonry construction refurbishment" Proceedings of the 40th IAHS World Congress on Housing, Funchal, Portugal, 2014.

[8] L. Pozza, F. Evangelista and R. Scotta "CLT used as seismic strengthener for existing masonry walls" Proceedings of the 17th Conference ANIDIS L'ingegneria sismica in Italia, Pistoia, Italy, 2017.

[9] I. Giongo, D. Dizhur, R. Tomasi and J. Ingham "In-situ testing of wall-to-diaphragm shear transferring connections in an existing clay brick URM building" Proceedings of the 9th International Masonry Conference, Guimarães, Portugal, 2014.

[10] N. Gattesco and M. Del Piccolo "Shear transfer between concrete members and stone masonry walls through driven dowels" *International Journal of Earthquake Engineering and Engineering Seismology*, vol. 12, no.1, 1998.

[11] R. Felicetti, N. Gattesco and E. Giuriani "Local phenomena around a steel dowel embedded in a stone masonry wall" *Materials and Structures*, vol. 30, pp 238-246, 1997.

[12] E. Giuriani, N. Gattesco and M. Del Piccolo "Experimental tests on the shear behaviour of dowels connecting concrete slabs to stone masonry walls" *Materials and Structures*, vol. 26, pp 293-301, 1993.

[13] ASTM C67-14: Standard test method for sampling and testing brick and structural clay tile. ASTM International, West Conshohocken, PA, USA, 2014.

[14] Italian Technical Approval CIT n.03/2013, Pannello in compensato di tavole RUBNER HOLZBAU, 2013.

[15] German Technical Approval Z-9.1-842, STEICOLVL R, STEICO LVL RS, STEICOLVL RL and STEICOLVL X – Laminated Veneer Lumber made of spruce, 2017.

[16] German Technical Approval Z-9.1-838, Board BauBuche S/Q – Laminated Veneer Lumber made of beech, 2015.

[17] European Technical Assessment ETA-05/0010, HECO MULTI-MONTI MMS Concrete screw for use in concrete, 2015.

[18] European Technical Assessment ETA-15/0352, Fischer concrete screw ULTRACUT FBS II Adjustable concrete screw, 2016.

[19] German Technical Approval Z-21.1-1879 HECO MULTI-MONTI TCC Timber Connect, 2014.

[20] European Committee for Standardization, EN 26891: Timber structures – Joints made with mechanical fasteners – General principles for the determination of strength and deformation characteristics, CEN, Brussels, Belgium, 1991.

[21] European Committee for Standardization, EN 12512: Timber structures – Test methods – Cyclic testing of Joints made with mechanical fasteners, CEN, Brussels, Belgium, 2001.

[22] ASTM E2126 - Standard test methods for cyclic (reversed) load test for shear resistance of vertical elements of the lateral force resisting systems for buildings, ASTM E2126-11, ASTM International, Pennsylvania, United States, 2011.

[23] European Committee for Standardization, EN 12504-2: Testing concrete in structures – Part 2: Non-destructive testing – Determination of rebound number, CEN, Brussels, Belgium, 2012.

[24] J. Brozovsky and J. Zach "Evaluation of technical condition of masonry structures" Proceedings of the 15th International Brick and Block Masonry Conference, Florianopolis, Brazil, 2012.